Garrett Heinrich, Kana Meece, Sharon L. Wardlaw, and Domenico Accili

Preserved Energy Balance in Mice Lacking FoxO1 in Neurons of Nkx2.1 Lineage Reveals Functional Heterogeneity of FoxO1 Signaling Within the Hypothalamus

Diabetes 2014;63:1572–1582 | DOI: 10.2337/db13-0651

METABOLISM

Transcription factor forkhead box O1 (FoxO1) regulates energy expenditure (EE), food intake, and hepatic glucose production. These activities have been mapped to specific hypothalamic neuronal populations using cell type–specific knockout experiments in mice. To parse out the integrated output of FoxO1-dependent transcription from different neuronal populations and multiple hypothalamic regions, we used transgenic mice expressing Cre recombinase from the *Nkx2.1* promoter to ablate loxP-flanked *Foxo1* alleles from a majority of hypothalamic neurons (Foxo1KO$^{Nkx2.1}$ mice). This strategy resulted in the expected inhibition of FoxO1 expression, but only produced a transient reduction of body weight as well as a decreased body length. The transient decrease of body weight in male mice was accompanied by decreased fat mass. Male Foxo1KO$^{Nkx2.1}$ mice show food intake similar to that in wild-type controls, and, although female knockout mice eat less, they do so in proportion to a reduced body size. EE is unaffected in Foxo1KO$^{Nkx2.1}$ mice, although small increases in body temperature are present. Unlike other neuron-specific *Foxo1* knockout mice, Foxo1KO$^{Nkx2.1}$ mice are not protected from diet-induced obesity. These studies indicate that, unlike the metabolic effects of highly restricted neuronal subsets (proopiomelanocortin, neuropeptide Y/agouti-related peptide, and steroidogenic factor 1), those of neurons derived from the Nkx2.1 lineage either occur in a FoxO1-independent fashion or are compensated for through developmental plasticity.

The physiological relevance of cerebral insulin action remains incompletely understood (1,2). The insulin receptor is expressed throughout the brain (3), and genetic manipulation of insulin receptors and components of the insulin signaling pathway has resulted in phenotypes of altered body weight (4), fertility (4) and counterregulatory response to hypoglycemia (5,6). We have previously shown that hypothalamic insulin receptors are implicated in the regulation of hepatic glucose production (HGP) and energy expenditure (EE) (7). Insulin signaling through insulin receptor substrate 2 in the brain (8) leads to the activation of phosphatidylinositol triphosphate kinase (9), where convergence with the leptin signaling pathway occurs. A common effector of both insulin and leptin signaling is forkhead box O1 transcription factor (FoxO1) (10,11).

Various neuron type–specific manipulations of FoxO1 have resulted in clearly defined roles of FoxO1 in the actions of insulin and leptin. Both FoxO1 and the leptin-responsive transcription factor signal transducer and activator of transcription 3 regulate key promoters in orexigenic agouti-related peptide (AgRP) and anorexigenic proopiomelanocortin (POMC) neurons (12), and delivering constitutively active FoxO1 to the hypothalamus increases food intake and body weight (13,14). Within AgRP neurons, FoxO1 affects both eating behavior and the ability of insulin to regulate HGP, and indirect evidence implicates

Berrie Diabetes Center, Department of Medicine, College of Physicians & Surgeons, Columbia University, New York, NY

Corresponding author: Domenico Accili, da230@columbia.edu.

Received 23 April 2013 and accepted 26 January 2014.

This article contains Supplementary Data online at http://diabetes.diabetesjournals.org/lookup/suppl/doi:10.2337/db13-0651/-/DC1.

the orphan G-protein–coupled receptor Gpr17 as a FoxO1 target responsible for its orexigenic effects (15), in addition to neuropeptide AgRP (12) and neuropeptide Y (Npy) (13). Within POMC neurons, FoxO1 enhances food intake by decreasing the processing of POMC-derived anorexigenic peptides through inhibition of carboxypeptidase E expression (16). Outside the arcuate nucleus, FoxO1 decreases EE and increases transcription of steroidogenic factor 1 in the ventral medial nucleus of the hypothalamus (VMH) (17). From these data, the overarching function of FoxO1 in the hypothalamus appears to be anabolic.

While these data provide a necessary anatomic-functional map of FoxO1 actions, they do not address the broader question of the overall role of FoxO1 in vivo. To fill this gap in knowledge, we sought to determine whether combined inactivation of FoxO1 in multiple neuronal types, as would be expected to occur in response to feeding, would enhance the anorexigenic effects of FoxO1 removal from individual cell populations. To accomplish this goal, we used mice expressing Cre recombinase throughout a majority of hypothalamic neurons by way of the *Nkx2.1* promoter. This transgenic line allows the expression of Cre recombinase within multiple cellular subtypes within the hypothalamus (18). Nkx2.1-Cre is expressed as early as embryonic day 10.5 (19,20) and is expressed in arcuate Npy and POMC neurons (21). We report here that mice with a genetic knockout of FoxO1 in the hypothalamus display mild decreases in body weight early in life that normalize as compensatory mechanisms exert their effects with age.

RESEARCH DESIGN AND METHODS

Maintenance and Care of Mouse Colony

Mice were housed in a specific pathogen–free animal facility, fed Picolab diet 5053 (Purina, Richmond, IN) or D124921 60% high-fat diet (HFD) (Research Diets, New Brunswick, NJ), and kept under a 12-h light/dark cycle. Nkx2.1-Cre mice were obtained from The Jackson Laboratory (Bar Harbor, ME) and backcrossed with mice having a C57BL/6J background for eight generations. Mice with loxP-flanked FoxO1 alleles have been previously described (22). All procedures were approved by the institutional animal care and utilization committee at Columbia University.

Real-Time PCR

Total RNA was isolated using the PerfectPure RNA Tissue Kit (5Prime, Gaithersburg, MD), and cDNA was made using qScript (Quanta Biosciences, Gaithersburg, MD), both according to the manufacturer's instructions. Real-time quantitative PCR (qPCR) was performed using GoTaq qPCR master mix (Promega, Madison, WI) on a C1000 Thermal Cycler with a CFX96 Real Time PCR Detection System (Bio-Rad, Hercules, CA). Pooled samples were used to generate serial 1:4 dilutions for standard curves. Primer sequences are available upon request.

Tissue RT-PCR

Total RNA was isolated using the PerfectPure RNA tissue kit (5Prime), and complimentary DNA was made using qScript (Quanta Biosciences)—both according to the manufacturers' instructions as described above. cDNA was added to the FoxO1 primers previously described (22) and was mixed with KAPA 2 × 2G Fast ReadyMix with dye (Kapa Biosystems, Woburn, MA). PCR was performed with the following program: 95°C for 4 min (1 cycle), 94°C for 30 s, 58°C for 30 s, 72°C for 45 s (38 cycles), 72°C for 10 min (1 cycle), and 4°C to finish. Electrophoresis was performed on a 2% agarose gel, and ethidium bromide staining was visualized by ultraviolet light.

Metabolic Cages and Body Composition

Mice were acclimated for 2 days in cages, and indirect calorimetry, activity, and food intake were measured during the light and dark cycles using the LabMaster Platform (TSE Systems, Chesterfield, MO) as previously described (15). For fasting-refeeding experiments, food was removed at 1700 h and replaced the next day at 0800 h.

Serum Analytes

Blood was removed from the tail of mice that were fasted overnight, ad libitum fed, or fasted overnight followed by 4-h refeeding. Blood was collected via heparinized capillary tubes and centrifuged to isolate serum. Serum was analyzed using mouse insulin ELISA (Mercodia, Uppsala, Sweden); leptin ELISA (Millipore, Billerica, MA); active ghrelin ELISA (Millipore, St. Charles, MO); and kits for cholesterol E (Wako, Richmond, VA), Infinity triglycerides (TGs) (Thermo Scientific, Middletown, VA), and nonesterified fatty acid (NEFA) (Wako) according to the manufacturer's instructions.

Neuropeptides

AgRP was measured by radioimmunoassay (RIA) using an antibody (provided by Dr. Gregory Barsh, Stanford University School of Medicine, Stanford, CA) directed at the COOH-terminal end of the molecule. The RIA was performed as previously described using synthetic human $AgRP_{83–132}$ for the standard and iodinated tracers (Phoenix Pharmaceuticals, Burlingame, CA) (23). Npy was measured with an RIA kit (Phoenix Pharmaceuticals), and α-melanocyte–stimulating hormone (α-MSH) and β-endorphin protein (β-Ep) were measured as previously described (16,23).

Immunohistochemistry and Microscopy

Liver tissue was fixed in formalin overnight, transferred to 70% ethanol, and paraffin embedded. Sections were cut to 5 μm, and hematoxylin-eosin (H-E) staining was performed. Brightfield images were taken using a Nikon eclipse E400 microscope. For brain tissue, mice were perfused with PBS followed by 4% paraformaldehyde. Brains were removed and fixed in 4% paraformaldehyde overnight, followed by

placement into 30% sucrose in PBS solution for 2 days. Free-floating sections were cut to 20 μm using a cryostat and mounted onto glass slides using Prolong Gold antifade reagent (Life Technologies, Grand Island, NY). Fluorescent images were obtained using either a Nikon Eclipse 80i microscope with images merged using Adobe Photoshop CS4 or a Zeiss LSM710 Confocal microscope with images merged using Zen 2011 software (Carl Zeiss MicroImaging, Thornwood, NY). Antibodies used were for FoxO1 (C29H4; Cell Signaling Technology, Danvers, MA), Nkx2.1/Ttf1 (rabbit ab76013, mouse ab140245; Abcam, Cambridge, MA), and Npy (ab30914; Abcam).

Body Temperature and Cold Exposure

Following overnight fasting at room temperature, body temperature was measured rectally using Precision Thermometer 4600 (YSI, Yellow Springs, OH). Mice were then placed at 4°C for 4 h, and temperature was remeasured while mice remained under acute cold exposure.

Liver TGs and Cholesterol

Liver tissue was homogenized and TGs and cholesterol were isolated via extraction as previously reported (24). TGs were measured with Infinity Triglycerides reagent (Thermo Scientific), and cholesterol was measured with a cholesterol E kit (Wako).

Statistics

Experiments were quantitated by two-tailed Student *t* test or one-way ANOVA using Prism software (GraphPad Software, La Jolla, CA). Results are presented as means ± SEM, and statistical significance is defined as $P < 0.05$.

RESULTS

Generation of Mice Lacking FoxO1 in Nkx2.1 Neurons

To probe the function of FoxO1 in the hypothalamus, we generated a conditional null allele by crossing *Foxo1*$^{lox/lox}$ with Nkx2.1-Cre mice. To assess recombination, we introduced a *Rosa26-Tomato* reporter allele and surveyed fluorescence patterns in the central nervous system. We observed diffuse fluorescence in the hypothalamus (Supplementary Fig. 1*A*) (18), as well as in the hippocampus and cortex (Supplementary Fig. 1*B*), as reported (http://cre.jax.org/Nkx2/Nkx2.html) (18). Nkx2.1-Cre was expressed in tanycytes lining the third ventricle but not in glial cells (Supplementary Fig. 1*C*). Deletion of FoxO1 did not result in compensatory increases in mRNA encoding other isoforms, *Foxo3a* and *Foxo4* (Supplementary Fig. 2*A*). Double immunofluorescence revealed colocalization of FoxO1 and Nkx2.1 protein in many neurons, as well as neurons independently labeled with either FoxO1 or Nkx2.1 (Supplementary Fig. 2*B*). Expression of the Nkx2.1-Cre recombinase decreased the levels of Foxo1 in Nkx2.1-labeled cells. Reverse transcription of RNA isolated from peripheral tissues followed by PCR amplification of the resulting cDNA revealed Nkx2.1-Cre expression in hypothalamus and lung but not in other organs (Supplementary Fig. 2*D*).

Characterization of Foxo1KO$^{Nkx2.1}$ Mice

Starting as early as 6 weeks of life, Foxo1KO$^{Nkx2.1}$ mice of both sexes weighed less than wild-type (WT) counterparts (Fig. 1*A* and *B*). In males, body weights of Foxo1KO$^{Nkx2.1}$ mice caught up with WT mice by 5 months of age. The convergence of body weights in male Foxo1KO$^{Nkx2.1}$ mice at 5 months of age could be due to compensatory mechanisms, such as decreasing numbers of POMC neurons, as we have reported in a different model of FoxO1 ablation (25). In males, the transient decrease of body weight is due to a proportional as well as an absolute decrease of fat mass, while the proportion of lean mass is higher as measured at 3 months of age (Fig. 1*C*, *D*, *F*, and *G*). Fluid mass was not affected in Foxo1KO$^{Nkx2.1}$ mice (Fig. 1*E* and *H*). Female Foxo1KO$^{Nkx2.1}$ mice also showed a decrease of fat mass, though not a significant decrease, and a larger decrease of lean mass, both of which were proportional to the decreased body weight (Supplementary Fig. 3).

We did not observe changes in metabolic parameters. Two-month-old Foxo1KO$^{Nkx2.1}$ mice have normal fasting and ad libitum–fed glucose levels (Table 1). There are no differences in serum insulin, TG, or free fatty acid (FFA) levels between WT and Foxo1KO$^{Nkx2.1}$ mice. Fasted serum levels of these metabolites are also similar in 7-month-old mice (Supplementary Fig. 4).

EE Studies

We postulated that the decreased body weight was at least partly due to increased EE in Foxo1KO$^{Nkx2.1}$ mice because altered FoxO1 expression in steroidogenic factor 1 neurons in the VMH leads to increases in EE (17). We analyzed Foxo1KO$^{Nkx2.1}$ mice using metabolic cages for indirect calorimetry and food intake measurements during the period (at 4 months of age) in which male Foxo1KO$^{Nkx2.1}$ mice remain lighter in this cohort (body weight 23.52 ± 1.47 vs. 25.29 ± 0.96 g) and lean (body fat 7.8 ± 0.5 vs. 9.1 ± 0.2%). However, measurements of respiratory exchanges demonstrated similar levels of V_{CO_2} and V_{O_2} between WT and Foxo1KO$^{Nkx2.1}$ mice in either the dark or the light phases of the light cycle (Fig. 2*A* and *B*). The 12-h respiratory exchange rates and locomotor activity levels were also similar (Fig. 2*C* and *D*). To study metabolic flexibility in substrate use, we fasted mice overnight and then refed them. Neither V_{CO_2} nor V_{O_2} was different between WT and Foxo1KO$^{Nkx2.1}$ mice in this experiment (Fig. 2*E* and *F*). Both groups of animals dropped their respiratory quotient similarly following fasting and rebounded equally upon refeeding (Fig. 2*G*). Female Foxo1KO$^{Nkx2.1}$ mice exhibited the same substrate use as males and showed no differences from WT controls (Supplementary Fig. 5).

Food Intake Studies

With no discernible differences in EE, we ascertained the role of food intake in the leanness of Foxo1KO$^{Nkx2.1}$ mice. Male mice exhibited normal absolute and body

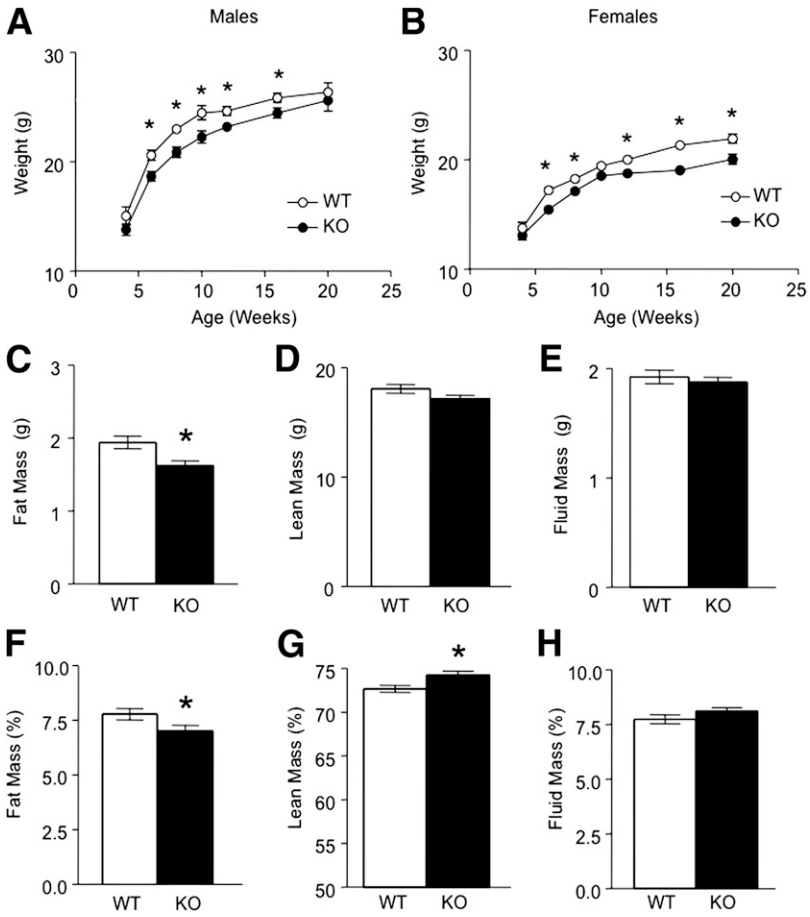

Figure 1—Growth curves. Body weights of 4- to 20-week-old male (*A*) and female (*B*) mice ($n > 10$ for each genotype). Total fat mass (*C*), lean mass (*D*), and fluid mass (*E*) in 3-month-old male mice as measured by magnetic resonance imaging ($n \geq 18$). Fat mass (*F*), lean mass (*G*), and fluid mass (*H*) shown as the percentage of total body weight. All results represent means ± SEM. *$P < 0.05$. KO, knockout.

weight–normalized food intake (Fig. 3*A* and *B*). Female Foxo1KO$^{Nkx2.1}$ mice, on the other hand, exhibited decreased overall food intake but normal intake proportional to their decreased size (Fig. 3*C* and *D*). In both males and females, rebound food intake after an overnight fast mirrored ad libitum food intake, with no difference in males (Fig. 3*E* and *F*) but weight-proportional decreases in females (Fig. 3*G* and *H*).

Table 1—Metabolic parameters

Parameters	*n*	WT mice	Foxo1KO$^{Nkx2.1}$ mice
Fasting glucose (mg/dL)	16	90 ± 5	94 ± 4
Fed glucose (mg/dL)	16	157 ± 6	163 ± 6
Fasting insulin (ng/mL)	5	0.48 ± 0.15	0.40 ± 0.13
TGs (mg/dL)	6	36 ± 4	42 ± 4
FFAs (mEq/L)	5	0.78 ± 0.06	0.89 ± 0.06

Data are means ± SEM in fasted or refed animals (N = X for each genotype). mEq, milliequivalent.

FoxO1 regulates the transcription of anorexigenic and orexigenic genes, as well as enzymes that process the neuropeptide products of those genes (12,13,16). While anorexigenic genes *Agrp* and *Npy* significantly decreased in male Foxo1KO$^{Nkx2.1}$ mice, there were no differences in *POMC* levels (Fig. 4*A*). Since the decreases in AgRP and Npy were ~50%, we postulated that Nkx2.1-Cre may not target all AgRP/Npy neurons, consistent with Nkx2.1-Cre–driven green fluorescent protein (GFP) reporter colocalization studies (21). However, previous use of the Nkx2.1-Cre revealed nearly complete targeting of leptin-sensitive neurons, as visualized by reductions in phosphorylated signal transducer and activator of transcription 3 upon deletion of the leptin receptor (18). To quantify the proportion of AgRP/Npy neurons targeted by the Nkx2.1-Cre, we introduced the Npy-GFP reporter into the WT and Foxo1KO$^{Nkx2.1}$ mice. We found virtually no Npy-GFP in the hypothalamus of Foxo1KO$^{Nkx2.1}$ mice (Fig. 4*B*), though Npy-GFP was observed in other parts of the brain such as the cortex (Supplementary Fig. 6*A*). Of note, the Nkx2.1-Cre (as visualized by inclusion of the Tomato reporter) did not colocalize with Npy-GFP outside of the hypothalamus. The Tomato reporter under Nkx2.1-Cre served as evidence of

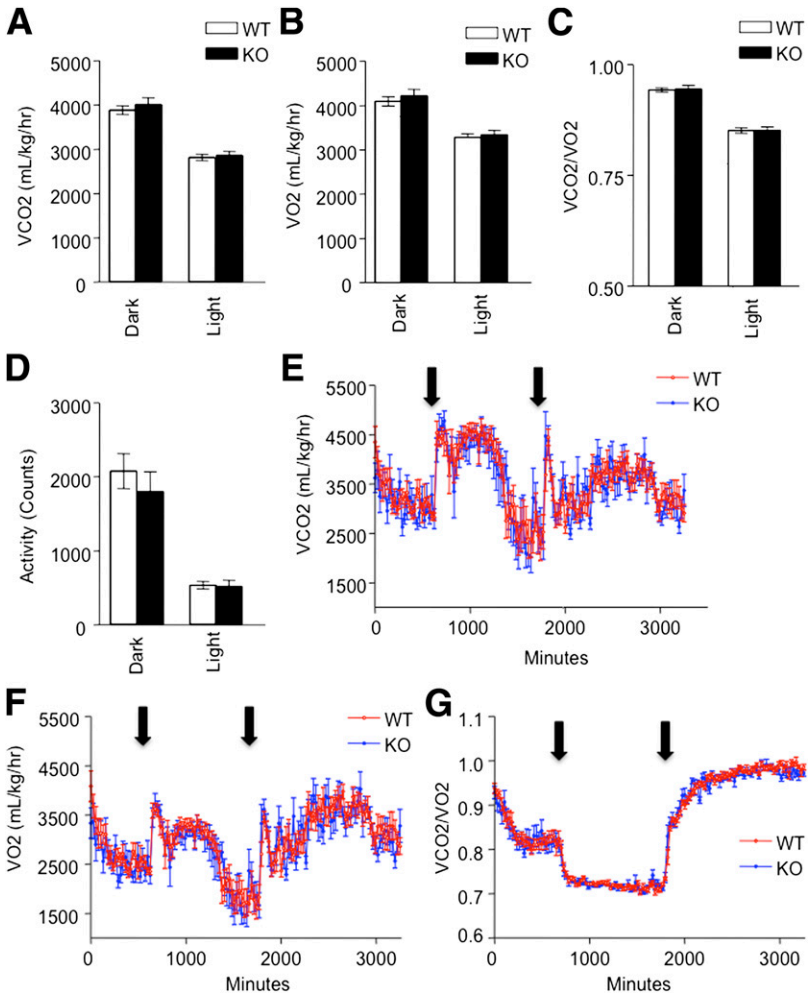

Figure 2—Energy balance in 4-month-old male mice. *A–D*: Ad libitum–fed animals. V_{CO_2} (*A*) and V_{O_2} (*B*) during a representative 12-h dark/light cycle. Respiratory exchange ratio (*C*) and locomotor activity (*D*) during a representative 12-h dark/light cycle. *E–G*: Fasting/refeeding experiments. V_{CO_2} (*E*), V_{O_2} (*F*), and respiratory exchange ratio (*G*) before and after fasting and following refeeding in 26-min increments. Data show means ± SEM. hr, hour; KO, knockout.

Cre-driven recombination within the hypothalamus, and Npy-GFP in nonhypothalamic areas provided evidence of proper genetic cross and sufficient GFP fluorescence for detection.

With the dramatic decrease in Npy-GFP expression in Foxo1KO$^{Nkx2.1}$ mice, we hypothesized that, whereas *Agrp/Npy* transcripts appeared decreased but still present in the hypothalamus, the protein was reduced or unstable. We measured levels of AgRP and Npy neuropeptides and found significant decreases that correlated with transcript levels (Fig. 4*C*). Levels of POMC-produced neuropeptides α-MSH and β-Ep were not altered in the Foxo1KO$^{Nkx2.1}$ mice, which is consistent with normal *POMC* transcript levels. The amount of Npy protein present in the arcuate nucleus and paraventricular nucleus revealed persistent levels in Foxo1KO$^{Nkx2.1}$ mice that did not match the difference in the Npy-GFP reporter (Supplementary Fig. 6*B*). We considered that Npy-GFP reporter activity may be compromised by the loss of a cofactor that binds to the Npy promoter fragment affected by insertion of the transgene; thus, we looked at alternate signaling pathways that may interact with FoxO1 on the Npy promoter. The ghrelin receptor is located in hypothalamic AgRP/Npy neurons and elicits a similar orexigenic effect upon stimulation by ghrelin (26). But we did not observe differences in serum levels of active ghrelin after either fasting or refeeding (Fig. 4*D*), and we also did not find differences in ghrelin receptor transcript or protein levels (data not shown).

Foxo1KO$^{Nkx2.1}$ Mice Are Not Protected From Diet-Induced Obesity

Given the transient decrease of body weight in Foxo1KO$^{Nkx2.1}$ mice on a chow diet, we used a diet containing 60% fat (HFD) to determine whether hypothalamic loss of FoxO1 protects from diet-induced obesity. Male Foxo1KO$^{Nkx2.1}$ mice weighed less than WT mice at the start of the experiment, but the difference in body weight normalized on an HFD (Fig. 5*A*). HFD also normalized body composition differences between WT and Foxo1KO$^{Nkx2.1}$

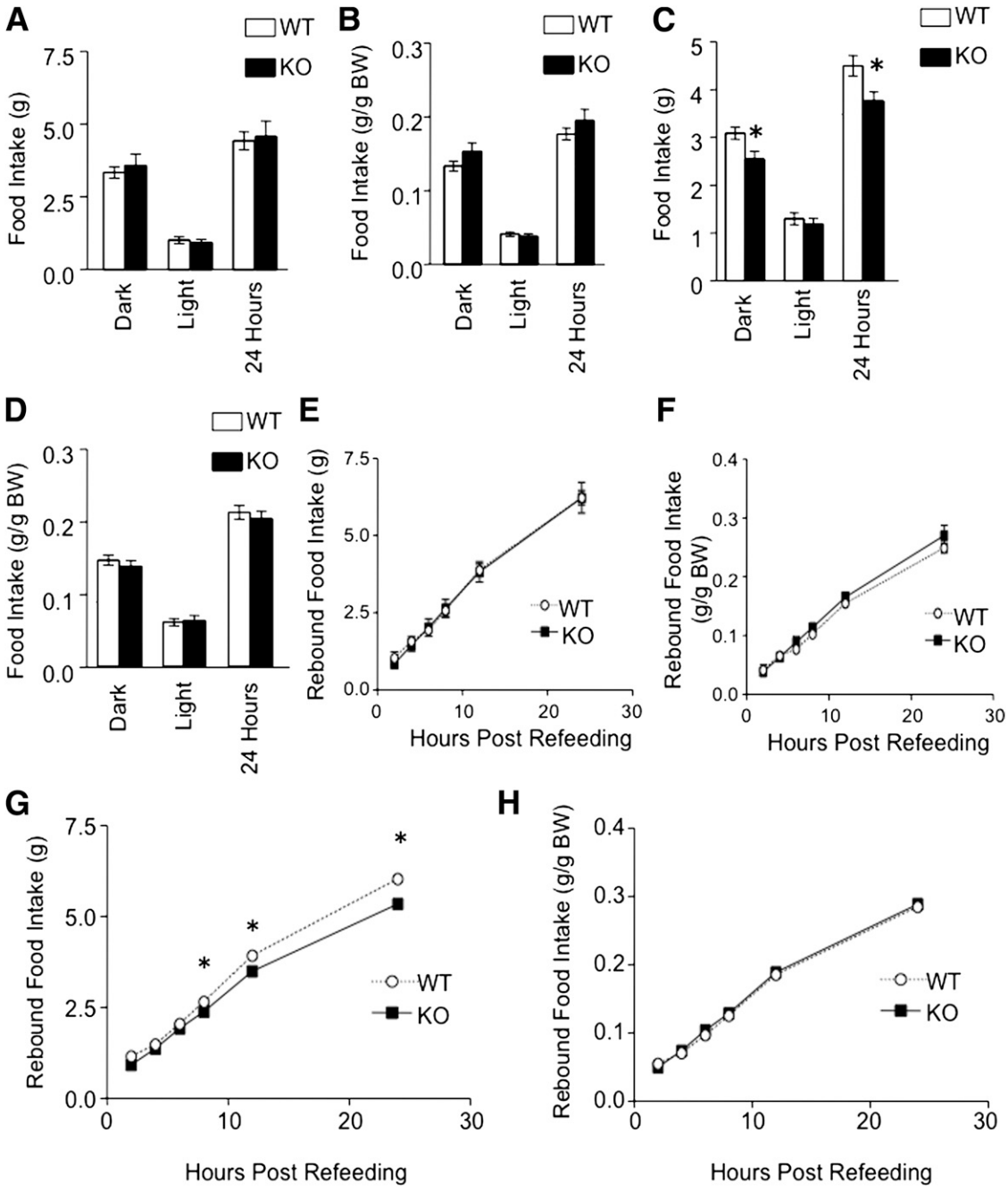

Figure 3—Assessment of food intake. *A*: Total food intake of 4-month-old male mice ($n \geq 7$) during the 12-h dark/light cycle and over 24 h. *B*: Food intake normalized by body weight during 12-h dark/light cycle and over 24 h. *C*: Total food intake of 4-month-old female mice during the 12-h dark/light cycle and over 24 h. *D*: Food intake normalized by female body weight during 12-h dark/light cycle and over 24 h. *E*: Total food intake in males over 24 h following overnight fast. *F*: Food intake in males after overnight fast normalized by body weight. *G*: Total food intake in females over 24 h following overnight fast. *H*: Food intake in females after overnight fast normalized by body weight. Data show means ± SEM. *$P < 0.05$. BW, body weight; KO, knockout.

mice (Supplementary Table 1), abolishing differences in fat mass and lean mass content, as seen in younger mice. Foxo1KO$^{Nkx2.1}$ mice were slightly shorter than WT mice at 5 months of age, and the difference reached statistical significance by 10 months (Fig. 5*H* and *I*). An HFD increased the body length of mice of both genotypes to the same extent.

Foxo1KO$^{Nkx2.1}$ mice exhibited a slight but not significant decrease in fasting glucose levels on regular chow and HFD (Fig. 5*B*). We saw no differences in fasting serum insulin levels (Fig. 5*C*). While HFD produced a large increase in fasting leptin levels compared with regular diet, it resulted in no differences between Foxo1KO$^{Nkx2.1}$ and WT mice (Fig. 5*D*). Serum cholesterol levels followed

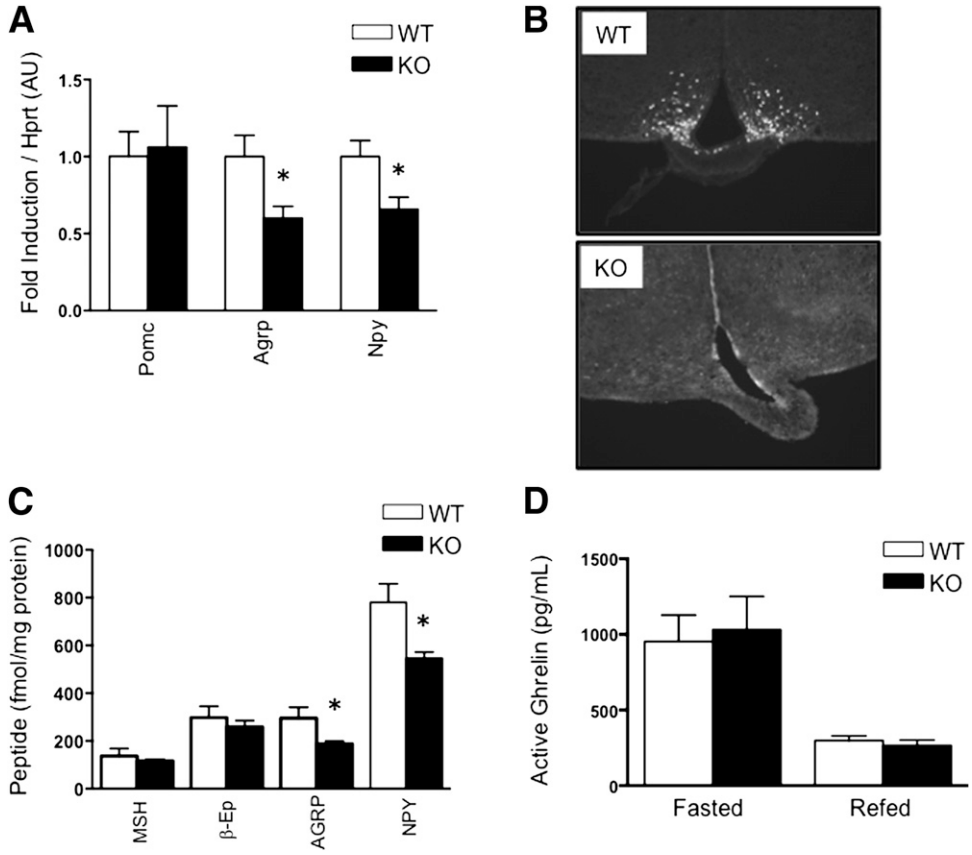

Figure 4—Hypothalamic neuropeptides. *A*: qPCR measurement of hypothalamic neuropeptide mRNA in overnight-fasted, 5-month-old male WT and Foxo1KO$^{Nkx2.1}$ mice ($n \geq 7$). *B*: Npy-GFP expression in arcuate nucleus of overnight fasted mice. Representative image shown. *C*: Protein levels of α-MSH, β-Ep, AgRP, and Npy in hypothalamus of overnight fasted, 5-month-old male WT and Foxo1KO$^{Nkx2.1}$ mice ($n \geq 7$). *D*: Serum levels of active ghrelin following overnight fast or overnight fast followed by 4 h refeeding ($n \geq 5$). Results are presented as means ± SEM. *$P < 0.05$. Hprt, hypoxanthine guanine phosphoribosyl transferase; AU, arbitrary units; KO, knockout.

a similar pattern, being raised by HFD, but not differently so in the two genotypes (Fig. 5*E*). In contrast, we saw a slight elevation in serum levels of TGs in HFD-fed Foxo1KO$^{Nkx2.1}$ mice compared with WT mice (Fig. 5*F*). Serum levels of FFAs were slightly decreased on HFD, but the differences were not statistically significant (Fig. 5*G*).

Neurons located in the dorsomedial hypothalamus project to brown adipose tissue and are implicated in the acute thermogenic response to cold exposure (27). Impaired leptin signaling in Nkx2.1-expressing neurons can prevent this response in younger mice (19). We measured the body temperature of WT and Foxo1KO$^{Nkx2.1}$ mice at room temperature and found a trend toward increased body temperature in Foxo1KO$^{Nkx2.1}$ mice (Fig. 6*A*). These increases may represent thermogenesis, which would not be detected by indirect calorimetry and can account for the decreased fat content of Foxo1KO$^{Nkx2.1}$ mice. However, when we placed mice at 4°C for 4 h to test acute thermogenesis, we failed to see a difference between genotypes (Fig. 6*A*), indicating that the acute sympathetic response to leptin signaling is intact in Foxo1KO$^{Nkx2.1}$ mice. Brown adipose tissue morphology does not appear to be distinct in Foxo1KO$^{Nkx2.1}$ mice (Fig. 6*B*).

Finally, in the light of elevated plasma TG levels on HFD, we examined hepatic lipid content in WT and Foxo1KO$^{Nkx2.1}$ mice. However, total lipid content was similarly increased by HFD (Fig. 6*C*), and there were no differences in levels of either hepatic TGs (Fig. 6*D*) or total cholesterol in 10-month-old mice on regular chow (Fig. 6*E*). Glucose tolerance was normal in Foxo1KO$^{Nkx2.1}$ mice on regular chow (Supplementary Fig. 7).

DISCUSSION

We generated Foxo1KO$^{Nkx2.1}$ mice with ablation of FoxO1 in hypothalamic Nkx2.1 neurons. These mice are leaner and smaller than WT mice at a young age, but the lean phenotype normalizes with age. There are modest differences in food intake in female knockouts, while EE is similar between the two groups. Given that FoxO1 is a downstream effector of both insulin and leptin signaling, we expected that Foxo1KO$^{Nkx2.1}$ mice would be a model of constitutively active, or at least sensitized, insulin and leptin signaling in hypothalamic neurons. In rats, decreasing hypothalamic insulin receptors results in increased food intake, obesity, and anxiety-like behavior (28,29). A localized knockdown of insulin receptors or

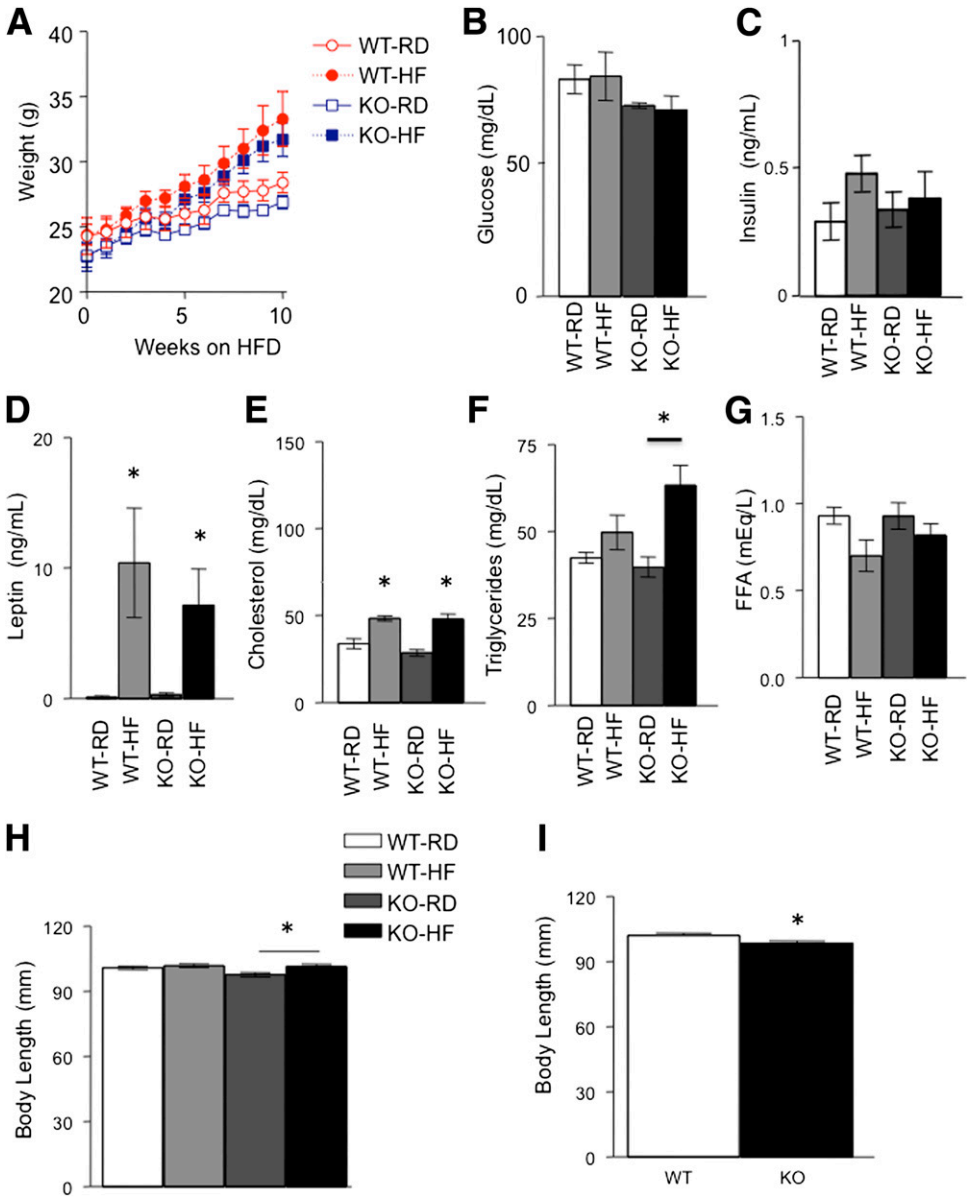

Figure 5—Metabolic effects of HFD. Body weight (*A*), whole-blood glucose (*B*), insulin (*C*), leptin (*D*), cholesterol (*E*), TGs (*F*), and FFAs (*G*) measured in serum of overnight-fasted male mice following a 10-week HFD (n = 5–8). *H*: Ano-nasal body length of males following HFD. *I*: Ano-nasal body length of 10-month-old male mice on regular chow diet (n = 5–8). Results are presented as means ± SEM. *$P < 0.05$. HF, high fat; KO, knockout; mEq, milliequivalent; RD, regular diet.

insulin signaling in the VMH does not affect body weight but increases glucagon secretion and results in insulin resistance (30,31). Although overall hypothalamic insulin receptor signaling inhibits HGP (32), genetic manipulations of selected hypothalamic neurons reveal opposing actions of insulin in AgRP neurons, where insulin signaling decreases HGP (33), versus POMC neurons, where insulin appears to increase HGP (7). In addition to HGP, insulin action in POMC neurons increases POMC neuron numbers in a FoxO1-dependent manner (25). The cell type–specific nature of insulin signaling among arcuate nucleus neurons may explain the phenotype of Foxo1KO$^{Nkx2.1}$ mice, where glucose levels and hepatic fat content appear to be normal.

Using targeted inactivation of FoxO1 in AgRP and POMC neurons, we have found FoxO1 to be important in the regulation of body weight and food intake (15,16). While the Nkx2.1-Cre mouse used in these studies does target these types of neurons, the overlap is not complete and is expected to leave FoxO1 intact in ~15% of adult POMC neurons and up to 45% of Npy neurons (21)—an expectation that is consistent with our finding of ~24% residual *Foxo1* mRNA within the hypothalamus (Supplementary Fig. 2*A*). Those neurons unaffiliated with the Nkx2.1 lineage may compensate for the decreased FoxO1 in other neurons and result in a mild phenotype. In addition, these data raise the possibility that the

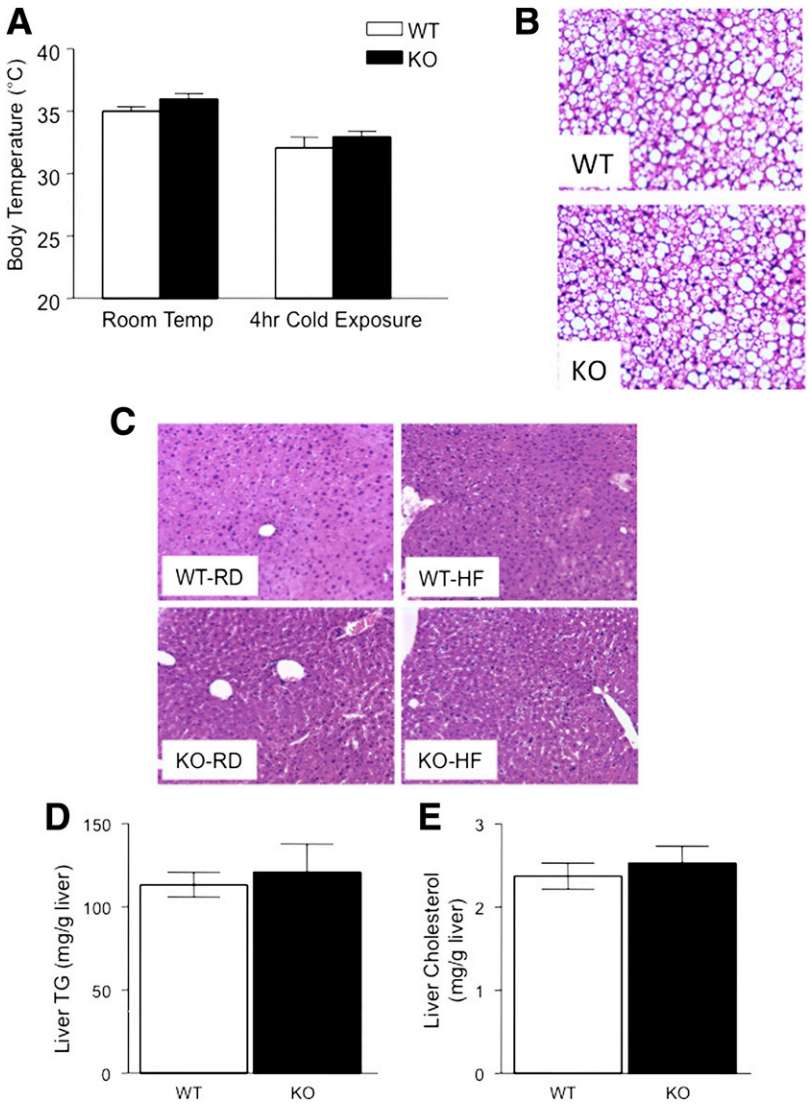

Figure 6—Brown adipose tissue and liver analysis. *A*: Rectal body temperature measured at room temperature and following 4 h of cold exposure at 4°C (n = 8). Results are shown as means ± SEM. *B*: H-E staining of brown adipose tissue at room temperature. We show a representative image. *C*: H-E staining of liver from WT and Foxo1KO$^{Nkx2.1}$ mice following regular chow or HFD. We show a representative image. TG (*D*) and total cholesterol (*E*) levels of 7-month-old male mice following overnight fasting. Results are shown as means ± SEM. HF, high fat; hr, hour; RD, regular diet; KO, knockout; Temp, temperature.

phenotype of FoxO1 knockouts driven by AgRP-Cre and POMC-Cre is in fact due not to the arcuate nucleus but to other subpopulations of such neurons in the paraventricular nucleus or brain stem (34). Alternatively, the activation of Nkx2.1-Cre may selectively reduce a pool of FoxO1 that is regulated by acetylation, not phosphorylation. Mice expressing constitutively acetylated FoxO1 (KR mice) exhibit an increased body weight and fat mass (35); therefore, the opposite body composition profile of the Foxo1KO$^{Nkx2.1}$ mice may be due in part to deletion of the pool of FoxO1 that undergoes acetylation within neurons of Nkx2.1 lineage.

The compensation in the overall bioenergetics profile of Foxo1KO$^{Nkx2.1}$ mice does not appear to affect body length. Interestingly, Kim et al. (17) found downregulation of a cluster of IGF-I–related genes when FoxO1 is deleted from the VMH, raising the possibility that Foxo1KO$^{Nkx2.1}$ mice have decreased IGF-I signaling, resulting in decreased length. We also hypothesized that another signaling pathway located within AgRP/Npy neurons, that of ghrelin through the growth hormone secretegogue receptor 1a, might be altered in the Foxo1KO$^{Nkx2.1}$ mice and affect body length (26). However, we did not find differences in ghrelin receptor transcript or protein level in Foxo1KO$^{Nkx2.1}$ mice (data not shown), and no compensatory changes in activated ghrelin levels in the serum were present.

The differences in male versus female fat composition may be due to differences in innervation of adipose tissue depots. Sexual dimorphism exists in the innervations of

abdominal and subcutaneous fat depots from the brain, including leptin-expressing and insulin receptor–expressing neurons (36). These connections may also contribute to the sexual dimorphism seen in body weight and food intake in mice lacking neuronal insulin receptors (4) or mice lacking Foxo1 in POMC neurons (16). Such dimorphism may reveal a need for sex-specific or individualized treatment when targeting the brain for weight reduction.

Decreases in AgRP and Npy are not sufficient alone to manifest body weight dysregulation when altered at an early age, but later deletion of AgRP/Npy in adults has powerful effects on food intake (37). This phenomenon suggests developmental compensation or redundant mechanisms existing within the neonatal brain that ensure a behavioral desire to eat and thrive. Even removal of both AgRP and NPY can be performed with little body weight or food intake phenotype results, though loss of both genes results in disruption of ghrelin signaling (38,39). As we could not identify changes in ghrelin receptor expression within the hypothalamus or circulating active ghrelin, the decrease in AgRP and Npy observed in the Foxo1KO$^{Nkx2.1}$ mice is not sufficient to elicit this disruption. In future studies, it will be of interest to explore this possibility by inducing a FoxO1 knockout in adult animals by way of inducible Cre-mediated recombination.

Acknowledgments. The authors thank Ana Flete, Timothy Guan, and Thomas Kolar (Columbia University) for excellent technical assistance; Lori Zeltzer, Hongxia Ren, and Li Qiang (Columbia University) for discussing the manuscript; and Hye-Lim Noh (Columbia University) for expertise with indirect calorimetry.

Funding. This research was supported by National Institutes of Health grants T32DK07328 and F32DK095541 (to G.H.), DK57539 (to D.A.), and DK63608 (to Columbia University Diabetes Research Center).

Duality of Interest. No potential conflicts of interest relevant to this article were reported.

Author Contributions. G.H. designed, executed, and analyzed the experiments and wrote the manuscript. K.M. executed the experiments. S.L.W. designed and reviewed the experiments. D.A. designed and reviewed the experiments and wrote the manuscript. D.A. is the guarantor of this work and, as such, had full access to all the data in the study and takes responsibility for the integrity of the data and the accuracy of the data analysis.

Prior Presentation. Parts of this study were presented in abstract form at the Neuronal Control of Appetite, Metabolism, and Weight Keystone Symposium, Banff, Alberta, Canada, 17–22 March 2013 and at the Challenges and Opportunities in Diabetes Research and Treatment Keystone Symposium, Vancouver, British Columbia, Canada, 12–17 January 2014.

References

1. Plum L, Schubert M, Brüning JC. The role of insulin receptor signaling in the brain. Trends Endocrinol Metab 2005;16:59–65
2. Levin BE, Sherwin RS. Peripheral glucose homeostasis: does brain insulin matter? J Clin Invest 2011;121:3392–3395
3. Unger JW, Livingston JN, Moss AM. Insulin receptors in the central nervous system: localization, signalling mechanisms and functional aspects. Prog Neurobiol 1991;36:343–362
4. Brüning JC, Gautam D, Burks DJ, et al. Role of brain insulin receptor in control of body weight and reproduction. Science 2000;289:2122–2125
5. Fisher SJ, Brüning JC, Lannon S, Kahn CR. Insulin signaling in the central nervous system is critical for the normal sympathoadrenal response to hypoglycemia. Diabetes 2005;54:1447–1451
6. Diggs-Andrews KA, Zhang X, Song Z, Daphna-Iken D, Routh VH, Fisher SJ. Brain insulin action regulates hypothalamic glucose sensing and the counterregulatory response to hypoglycemia. Diabetes 2010;59:2271–2280
7. Lin HV, Plum L, Ono H, et al. Divergent regulation of energy expenditure and hepatic glucose production by insulin receptor in agouti-related protein and POMC neurons. Diabetes 2010;59:337–346
8. Choudhury AI, Heffron H, Smith MA, et al. The role of insulin receptor substrate 2 in hypothalamic and beta cell function. J Clin Invest 2005;115:940–950
9. Xu AW, Kaelin CB, Takeda K, Akira S, Schwartz MW, Barsh GS. PI3K integrates the action of insulin and leptin on hypothalamic neurons. J Clin Invest 2005;115:951–958
10. Ernst MB, Wunderlich CM, Hess S, et al. Enhanced Stat3 activation in POMC neurons provokes negative feedback inhibition of leptin and insulin signaling in obesity. J Neurosci 2009;29:11582–11593
11. Sasaki T, Kitamura T. Roles of FoxO1 and Sirt1 in the central regulation of food intake. Endocr J 2010;57:939–946
12. Kitamura T, Feng Y, Kitamura YI, et al. Forkhead protein FoxO1 mediates Agrp-dependent effects of leptin on food intake. Nat Med 2006;12:534–540
13. Kim MS, Pak YK, Jang PG, et al. Role of hypothalamic Foxo1 in the regulation of food intake and energy homeostasis. Nat Neurosci 2006;9:901–906
14. Kim HJ, Kobayashi M, Sasaki T, et al. Overexpression of FoxO1 in the hypothalamus and pancreas causes obesity and glucose intolerance. Endocrinology 2012;153:659–671
15. Ren H, Orozco IJ, Su Y, et al. FoxO1 target Gpr17 activates AgRP neurons to regulate food intake. Cell 2012;149:1314–1326
16. Plum L, Lin HV, Dutia R, et al. The obesity susceptibility gene Cpe links FoxO1 signaling in hypothalamic pro-opiomelanocortin neurons with regulation of food intake. Nat Med 2009;15:1195–1201
17. Kim KW, Donato J Jr, Berglund ED, et al. FOXO1 in the ventromedial hypothalamus regulates energy balance. J Clin Invest 2012;122:2578–2589
18. Ring LE, Zeltser LM. Disruption of hypothalamic leptin signaling in mice leads to early-onset obesity, but physiological adaptations in mature animals stabilize adiposity levels. J Clin Invest 2010;120:2931–2941
19. Xu Q, Tam M, Anderson SA. Fate mapping Nkx2.1-lineage cells in the mouse telencephalon. J Comp Neurol 2008;506:16–29
20. Sussel L, Marin O, Kimura S, Rubenstein JL. Loss of Nkx2.1 homeobox gene function results in a ventral to dorsal molecular respecification within the basal telencephalon: evidence for a transformation of the pallidum into the striatum. Development 1999;126:3359–3370
21. Yee CL, Wang Y, Anderson S, Ekker M, Rubenstein JL. Arcuate nucleus expression of NKX2.1 and DLX and lineages expressing these transcription factors in neuropeptide Y(+), proopiomelanocortin(+), and tyrosine hydroxylase(+) neurons in neonatal and adult mice. J Comp Neurol 2009;517:37–50
22. Paik JH, Kollipara R, Chu G, et al. FoxOs are lineage-restricted redundant tumor suppressors and regulate endothelial cell homeostasis. Cell 2007;128:309–323
23. Breen TL, Conwell IM, Wardlaw SL. Effects of fasting, leptin, and insulin on AGRP and POMC peptide release in the hypothalamus. Brain Res 2005;1032:141–148
24. Qiang L, Lin HV, Kim-Muller JY, Welch CL, Gu W, Accili D. Proatherogenic abnormalities of lipid metabolism in SirT1 transgenic mice are mediated through Creb deacetylation. Cell Metab 2011;14:758–767
25. Plum L, Lin HV, Aizawa KS, Liu Y, Accili D. InsR/FoxO1 signaling curtails hypothalamic POMC neuron number. PLoS One 2012;7:e31487
26. Andrews ZB. Central mechanisms involved in the orexigenic actions of ghrelin. Peptides 2011;32:2248–2255
27. Zhang Y, Kerman IA, Laque A, et al. Leptin-receptor-expressing neurons in the dorsomedial hypothalamus and median preoptic area regulate sympathetic brown adipose tissue circuits. J Neurosci 2011;31:1873–1884

28. Obici S, Feng Z, Karkanias G, Baskin DG, Rossetti L. Decreasing hypothalamic insulin receptors causes hyperphagia and insulin resistance in rats. Nat Neurosci 2002;5:566–572
29. Grillo CA, Piroli GG, Kaigler KF, Wilson SP, Wilson MA, Reagan LP. Downregulation of hypothalamic insulin receptor expression elicits depressive-like behaviors in rats. Behav Brain Res 2011;222:230–235
30. Paranjape SA, Chan O, Zhu W, et al. Chronic reduction of insulin receptors in the ventromedial hypothalamus produces glucose intolerance and islet dysfunction in the absence of weight gain. Am J Physiol Endocrinol Metab 2011;301:E978–E983
31. Paranjape SA, Chan O, Zhu W, et al. Influence of insulin in the ventromedial hypothalamus on pancreatic glucagon secretion in vivo. Diabetes 2010;59:1521–1527
32. Obici S, Zhang BB, Karkanias G, Rossetti L. Hypothalamic insulin signaling is required for inhibition of glucose production. Nat Med 2002;8:1376–1382
33. Könner AC, Janoschek R, Plum L, et al. Insulin action in AgRP-expressing neurons is required for suppression of hepatic glucose production. Cell Metab 2007;5:438–449
34. Blouet C, Schwartz GJ. Hypothalamic nutrient sensing in the control of energy homeostasis. Behav Brain Res 2010;209:1–12
35. Banks AS, Kim-Muller JY, Mastracci TL, et al. Dissociation of the glucose and lipid regulatory functions of FoxO1 by targeted knockin of acetylation-defective alleles in mice. Cell Metab 2011;14:587–597
36. Adler ES, Hollis JH, Clarke IJ, Grattan DR, Oldfield BJ. Neurochemical characterization and sexual dimorphism of projections from the brain to abdominal and subcutaneous white adipose tissue in the rat. J Neurosci 2012;32:15913–15921
37. Luquet S, Perez FA, Hnasko TS, Palmiter RD. NPY/AgRP neurons are essential for feeding in adult mice but can be ablated in neonates. Science 2005;310:683–685
38. Qian S, Chen H, Weingarth D, et al. Neither agouti-related protein nor neuropeptide Y is critically required for the regulation of energy homeostasis in mice. Mol Cell Biol 2002;22:5027–5035
39. Chen HY, Trumbauer ME, Chen AS, et al. Orexigenic action of peripheral ghrelin is mediated by neuropeptide Y and agouti-related protein. Endocrinology 2004;145:2607–2612